Materials Science in Semiconductor Processing 130 (2021) 105819

Contents lists available at ScienceDirect

Materials Science in Semiconductor Processing

journal homepage: http://www.elsevier.com/locate/mssp

The relationship between structural and electrical properties of the post-deposition annealed Er_2O_3/n-Si hetero-structures

Aysegul Kahraman [a], Berk Morkoc [b], Ercan Yilmaz [c,d,*]

[a] Physics Department, Faculty of Arts and Sciences, Bursa Uludag University, 16059, Bursa, Turkey
[b] Physics Department, Engineering and Natural Sciences, Bursa Technical University, 16059, Bursa, Turkey
[c] Physics Department, Faculty of Arts and Sciences, Bolu Abant Izzet Baysal University, 14280, Bolu, Turkey
[d] Center for Nuclear Radiation Detector Research and Applications, Bolu Abant Izzet Baysal University, 14280, Bolu, Turkey

A B S T R A C T

This study presents comprehensive results on the structural modifications of Er_2O_3/n-Si hetero-structures under post-deposition annealing (PDA) and the effects of these changes on the electrical characteristics of the Al/Er_2O_3/n-Si/Al MOS capacitors. The Er_2O_3 films were grown on n-Si substrate with RF magnetron sputtering and annealed under nitrogen at RT, 300 °C, 500 °C, 600 °C, 700 °C. The increasing grain size of the films up to 300 °C did not show a significant change in other annealing temperatures. The erbium silicate content in the RT and 600 °C-Er_2O_3/n-Si interface is quite higher than those of 500 °C and 700 °C, while a silicate-like layer was not found at 300 °C. The highest dielectric constant (ε) value was obtained from the 500 °C-Er_2O_3 MOS capacitor due to the lowest oxygen deficient bond content. It was found that Q_{eff} values tend to increase as the oxygen concentration decreases in the film. It was determined that Er-Er oxygen deficient bonds may have acted as negative charge trap centers. Although the Er-M content in the 700 °C-Er_2O_3/n-Si is higher than that of 500 °C, lower Q_{eff} values were obtained from the 700 °C-Er_2O_3 MOS capacitor due to the higher Si-Si oxygen deficient bond content, which is most likely act as a positive charge trap center. It was concluded that the contributions of oxide trap and interface trap charges should be evaluated together in establishing a link between electrical characteristics and structural analyses.

1. Introduction

Many researches have been carried out for the use of high-k oxides as gate dielectrics with the aims of obtaining small sized CMOS, improving the sensitivity of pMOS dosimeters to low doses in recent years [1–4]. The rare earth oxides (REO) are widely used for some reasons such as high effective atomic number (Z_{eff}), high thermal stability with Si, excellent chemical properties, large band gap and conduction band offset, etc. [5–7]. The most important disadvantage of rare earth oxides is that their water vapour absorption properties (hygroscopic nature) are high, which can lead to decreased device reliability/degradation of electrical properties [8]. Especially hydrogen-related defects, which can act as a negative charge trap center, worsen the sensitivity of the radiation sensors as they cause undesirable shifts in the threshold voltage [9]. On the other hand, it is known that the oxygen deficient bond content is generally high in the rare earth oxides [8,10]. The thermal annealing is a widely used to reduce hydroxyl content and treat defect centers. However, this method brings some obstacles: i) some of the defects can turn into neutral electron trap centers without permanent treatment [11–13]. ii) Silicate-like interfacial layer can form during the annealing process, resulting in losses in the film's dielectric properties [14]. iii) There are studies showing that the leakage current is lower in the device with amorphous films compared to crystalline ones [15–17]. However, there is also research showing that the leakage current decreases with increasing grain size [18]. It is reported that the probability of formation of silicate during the post-deposition annealing (PDA) at the oxide/n-Si interface formed with Erbium (III) oxide (Er_2O_3) is lower compared to other rare earth oxides such as La_2O_3, Gd_2O_3 [6]. The radiation response of 500 °C-Er_2O_3 MOS capacitor was analysed in our previous study [19], and it was found that negative charges in the dose range of 4–16 Gy and positive charges in the dose range of 16–76 Gy were dominantly trapped in the structure. Determining which defect centers/defective bonds are formed after production and which loads are heavily trapped is critical for resolving these unstable behaviours observed in device performance. On the other hand, what kind of changes the annealing causes in the structure and their effect on the electrical properties should be determined in detail.

Kaya and Yilmaz [20] tried to link the electrical characteristics of the Er_2O_3 MOS capacitor with the XPS (X-ray photoelectron spectroscopy) data taken from the Er_2O_3/p-Si interface and reported that the reduced oxygen concentration with irradiation compared to Er was associated with positive charge traps. Kahraman et al. [21] examined the effects of

* Corresponding author. Physics Department, Faculty of Arts and Sciences, Bolu Abant Izzet Baysal University, 14280, Bolu, Turkey.
E-mail address: yilmaz@ibu.edu.tr (E. Yilmaz).

https://doi.org/10.1016/j.mssp.2021.105819
Received 23 November 2020; Received in revised form 11 March 2021; Accepted 14 March 2021
Available online 25 March 2021
1369-8001/

PDA on the structural properties of the Yb_2O_3/n-Si by taking the XPS spectra from both the film and the interface, and established a relation between the structural modifications and electrical properties. The obtained results revealed that in order to establish a strong link between the structural analyses and electrical characteristics, the structural properties of the oxide as well as interface should be examined in detail.

The aims of this study are: i) Determination of structural modifications of Er_2O_3/n-Si hetero-structures annealed at different temperatures by XRD (X-ray Diffraction) and XPS techniques, ii) Investigation of electrical properties of MOS capacitors produced with Er_2O_3 films annealed at RT (room temperature)-700 °C under nitrogen ambient, iii) Linking structural analysis with electrical results. To the best of our knowledge, for the first time, a relationship was established between the structural and electrical characteristics by considering the oxide and interface bond properties for the Er_2O_3/n-Si MOS structure in this study.

2. Experimental

The Er_2O_3 thin films were deposited on 6 inch n-type Si (100) substrate by RF magnetron sputtering system. Possible contamination on the wafer was removed following the RCA cleaning procedure. After the nitrogen-dried wafer and the Er_2O_3 target (the purity of 99.9%) were placed inside the vacuum chamber, the system pressure was reduced to 6×10^{-4} Pa. The plasma was ensured with the argon gas with the pressure of 1 Pa and flow rate of 16 sccm. After the system was operated at 300 W for 1 h to remove the possible contamination on the target, the shutters on the wafer were opened and the film deposition was carried out for 18 min. The thickness of thin films measured in the wavelength range of 400–840 nm by Angstrom Sun Spectroscopic Reflectometer was found around 118 nm. A part of the 6 inch Er_2O_3/n-Si structure was separated and the remaining part was divided into four parts, which were annealed at 300 °C, 500 °C, 600 °C, 700 °C in nitrogen ambient.

The XPS spectra of the Er_2O_3/n-Si structures were taken with Physical Electronics PHI 5000 VersaProbe (Monochromatic Al Kα X-ray radioactive source-1486.6 eV) at Middle East Technical University. The film etching was conducted with the Ar^+-1 keV sputtering. All spectra were corrected with reference to C 1s-284.8 eV. The XPS spectra were deconvoluted to G-L (Gaussian-Lorentzian) functions by using XPSPEAK 4.1 software [22]. The Lorentzian:Gaussian ratio for the oxide was lower than 20:80 [23].

Metal contacts of Er_2O_3 MOS capacitors were formed with DC magnetron sputtering system using Al target with the purity of 99.99%. A shadow mask with a diameter of 1.5 mm was used to create the front metal electrodes. The back of the Si wafer was completely covered with Al to prevent possible signal losses. The electrical characteristics of the device were measured with HIOKI-LCR meter at six different frequencies.

3. Results and discussion

3.1. Structural analyses

The XRD spectra of the 118 nm-thick Er_2O_3/n-Si hetero-structures taken in the diffraction angle range (2θ) of 20°-80° were given in Fig. 1. Due to the dominant Si peak observed at around 70° and no peak between 66°-80°, this part of the spectrum was not included in the figure. The planes in the spectra and phases of the films were determined by reference to the International Center for Diffraction Data (ICDD). The data complied with the cubic phase of Er_2O_3 determined by card no: 76–0159. Only the peak representing the reflection from the plane (222) was observed in the RT-Er_2O_3/n-Si hetero-structure, while the peaks of the (400), (440) and (622) were appeared with increasing annealing temperature in the spectra. No peaks indicating the any impurity were found in the all of the spectra. The grain sizes were calculated from the well-known Scherrer's expression [24] and the values were given in Table 1. While the lowest grain size was observed in the RT-Er_2O_3/n-Si

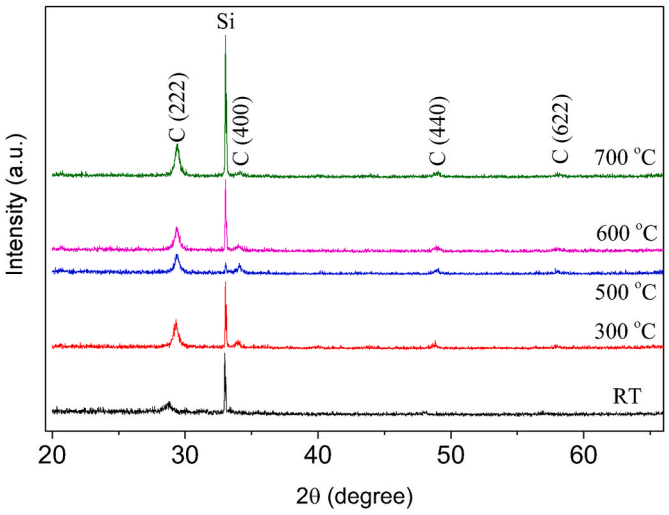

Fig. 1. XRD spectra of the Er_2O_3/Si structures annealed at RT, 300 °C, 500 °C, 600 °C, 700 °C.

Table 1
Grain sizes and oxygen deficient bond contents at the interface.

Annealing Temp. (°C)	Grain size (nm)	Er-O-Er (%)	Er-O-Si (%)	Si-O (%)	Er-Si (%)	Si-Si (%)
RT	18.7	50	25	25	36	64
300	24.0	100	–	–	–	–
500	22.5	93	3	4	–	–
600	24.2	50	29	21	26	74
700	22.5	91	4	5	–	–

structure, the values obtained in the annealing temperature range of 300 °C–700 °C were found quite close to each other.

The Si 2p, Er 4d, O 1s and C 1s XPS depth profiles were taken from the surfaces and eight different depths of the Er_2O_3/n-Si hetero-structures annealed at RT, 300 °C, 500 °C, 600 °C, 700 °C to investigate the chemical composition and bond properties. Since the amount of carbon is high on the surface of thin films, XPS data taken from this region was not used. No carbon or impurities were found in other layers of the films. The binding energy peaks of the Si 2p and Er MVV Auger electrons overlap in the Si 2p XPS spectrum of an Er-based oxide. The Si 2p, Er 4d and O 1s spectra taken from the annealed Er_2O_3/n-Si at RT, 300 °C, 500 °C, 600 °C and 700 °C are similar. Therefore, typical XPS

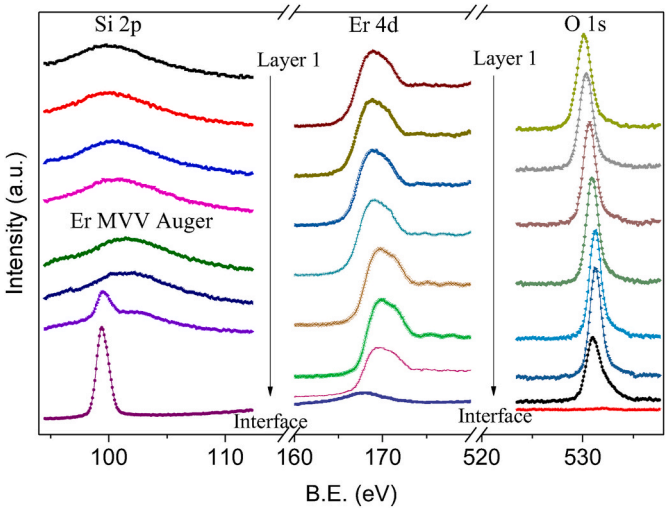

Fig. 2. Typical XPS spectra of the Si 2p, Er 4d and O 1s.

spectra were given in Fig. 2. The effect of Er MVV Auger electrons on Si 2p is evident, resulting in the observation of the Si in the atomic concentration data of the film. An Er_2O_3 film is expected to consist of 40% Er and 60% oxygen atoms.

The depth-dependent oxygen atomic concentration (A.C.) is shown in Fig. 3. After the sputtering time exceeded 36 min, the oxygen concentration in the next layer has changed around 1%, indicating that the film was completely etched and reached to Si wafer. The oxygen concentration is below 60% for all annealing conditions, indicating the presence of the Er-Er, Er-Si and Si-Si oxygen deficient bonds and formation of non-stoichiometric film. Some bonds may be broken under any external influence such as annealing or irradiation, and as a result elements such as N, O can be separated from the structure in gas form [25,26].

On the other hand, atomic concentrations may also be related to the uniformity of the film grown on a 6-inch wafer. The O concentration in the film can be given as 500 °C>700 °C > RT>300 °C>600 °C in descending order depending on the annealing temperature. The possible reason of the observation of the lowest O concentration at 600 °C is that the oxygen separates in gas form and does not re-join the bond. Identifying the content of these defects in each sample can help establish a link between structural and electrical characteristics. Fig. 4 shows typical Er 4d spectra taken from the film and the interface. The spectra taken from the films annealed at 300 °C, 500 °C, 600 °C, 700 °C are deconvoluted into two G-L functions, which are Er-Er and Er-O peaks centered at ~166.7 eV and ~168.9 eV, respectively (Fig. 4a) [8,27,28]. A third peak was added to the XPS spectra from the Er_2O_3 film annealed at room temperature, which is attributed to $Er(OH)_x$ centered at 167.72 eV (Fig. 4b) [8,29]. The lowest energy peak is assigned to Er-M (Er-Er and Er-Si bonds) at the interface for 300 °C, 500 °C, 600 °C, 700 °C, while the medium and highest energy peaks represent the Er-O and Er-O-Si bonds, respectively (Fig. 4c) [28,30,31]. It was not possible to separate the peaks assigned to hydroxyl species and silicate from each other, because the binding energies are very close to each other. The RT-interface may contain the $ErSi(OH)_x$. The Er-M/T ratio was obtained by dividing the Er-M peak area into the total area of the spectrum. The depth-dependent Er-M/T variation was given in Fig. 5. It can be said that the lowest Er-M values are obtained from the 500 °C-Er_2O_3/n-Si hetero-structure. The O 1s spectra taken from the RT-Er_2O_3/n-Si are deconvoluted into two G-L functions. The peaks centered at ~527.7 eV and ~530.1 eV are assigned to the oxygen in the lattice (O_L) and bonded oxygen species (O_b) such as oxygen defects, hydroxyl groups, respectively (Fig. 6a) [8,28,29,32]. The O_b/T ratio was calculated by dividing the O_b peak area by the total area of the spectrum. The content of bonded oxygen species ranging from 8% to 13% were found in the RT-Er_2O_3/n-Si. The O 1s XPS spectra

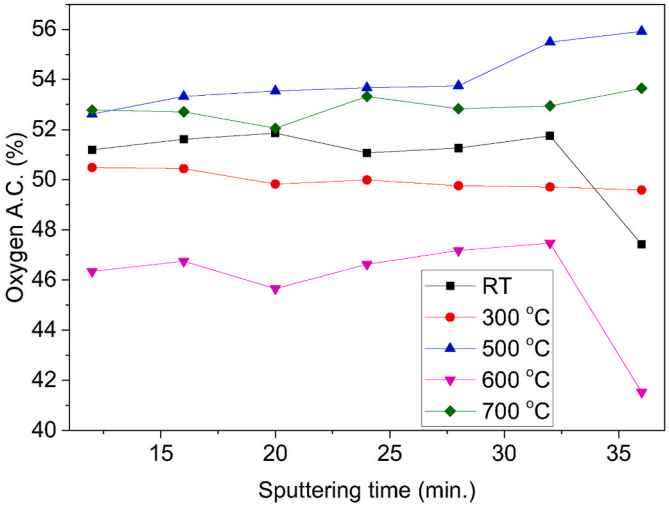

Fig. 3. Depth-dependent oxygen atomic concentration (A.C.).

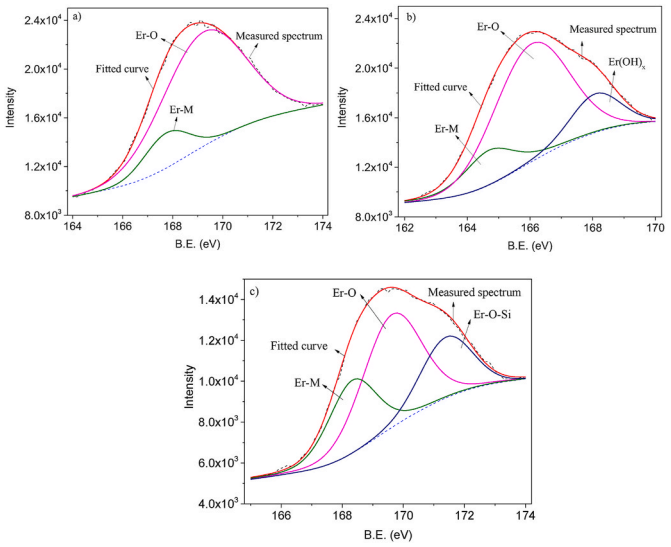

Fig. 4. Typical Er 4d spectra taken from a) film annealed at 300 °C–700 °C, b) film annealed at RT, c) interface annealed at 300 °C–700 °C.

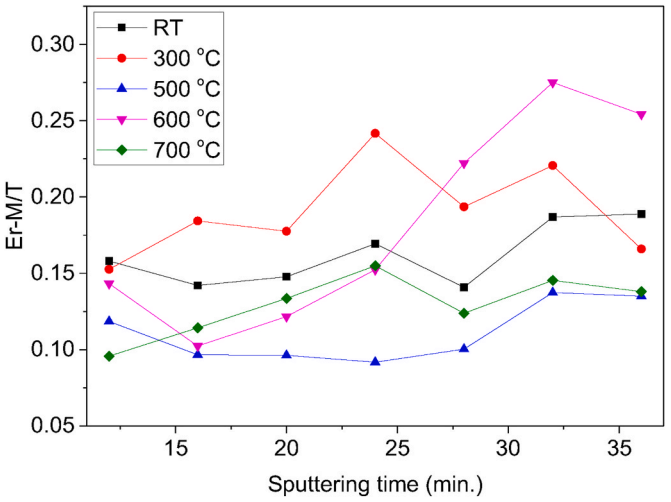

Fig. 5. Depth-dependent Er-M/T ratios.

taken from the Er_2O_3/n-Si interface for all annealing conditions are deconvoluted into three G-L functions. The low, medium and high energy peaks represent the Er-O-Er, and Er-O-Si and Si-O, respectively (Fig. 6b) [8,28,29,32]. The bonded oxygen species were not found in structures annealed at other temperatures except RT. Therefore, the peak attributed to Si-O at the interface in RT also includes the bonded oxygen types. The erbium silicate content at the interfaces was determined by dividing the area of the representing Er-O-Si to the total area of the O 1s spectrum (Table 1). While the erbium silicate content for RT and 600 °C is around 25% and 29%, respectively, the Er-O-Si content is lower than 5% in other Er_2O_3/n-Si interfaces annealed at 500 °C and 700 °C. The intensity of the silicate peak is quite weak at 300 °C. O 1s spectra taken from other layers of the films annealed at 300 °C, 500 °C, 600 °C, 700 °C were deconvoluted into a single peak attributed to Er-O-Er bond (Fig. 6c).

A typical Si 2p spectrum for the RT and 600 °C-interface was given in Fig. 7. The low and high energy peaks in the Si 2p spectra represent the Er-Si and Si-Si oxygen deficient bonds, respectively [31]. The Er-Si and Si-Si contents determined based on the peak areas were given in Table 1. Si 2p signal intensity is at a level that would not make it possible to make a healthy fit at 500 °C and 700 °C. However, the Si-Si signal intensity at

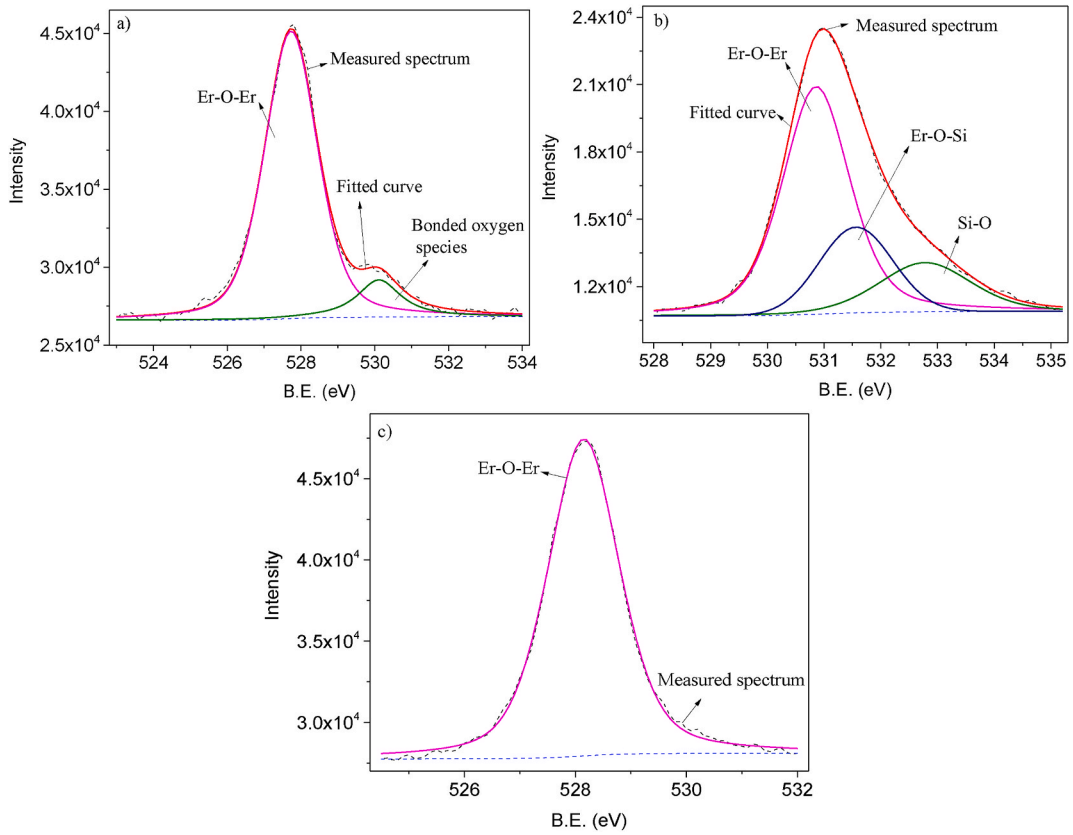

Fig. 6. Typical O 1s spectra taken from a) RT-film, b) interface, c) 300 °C, 500 °C, 600 °C, 700 °C-film.

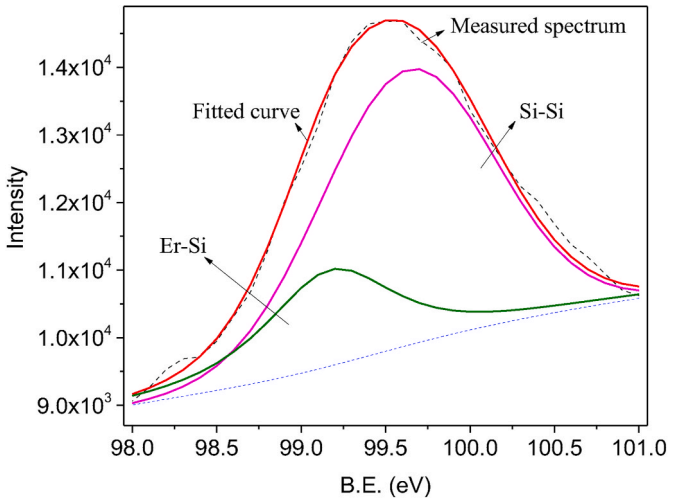

Fig. 7. Typical Si 2p spectra for the RT and 600 °C-interface.

the 700 °C is slightly higher than that of 500 °C.

Er-O-Er peaks in the Er 4d and O 1s spectra were taken as reference and the change in binding energies (B.E.) depending on depth was determined as shown in Fig. 8. Kao et al. [28] reported that the increase in binding energy in the Er 4d and O 1s spectra is associated with the preference of oxygen atoms to bond with Er atoms. On the other hand, it was mentioned in the same study that the increase in signal intensities is related to the development of the crystal properties of the film. The highest binding energy values in both Er 4d and O 1s spectra were observed in the annealed structure at 500 °C, which is compatible with the fact that the structure contains a higher rate of oxygen atoms than the annealed Er_2O_3/n-Si at other annealing temperatures. The lowest Er 4d and O 1s signal intensities were obtained from the RT-Er_2O_3/n-Si structure, which is consistent with the grain size values calculated from the XRD spectra (Fig. 9). The signal intensity of Er 4d was close to each other at 300 °C, 500 °C, 600 °C, 700 °C. The signal strength of O 1s exhibited a similar behaviour other than 300 °C. These results show that the crystal structure improves with the annealing temperature of 300 °C, which is compatible with the grain size data. In general, as the Si layer is approached, an increase in spectrum binding energies can be observed, which is related to the high electronegativity of Si compared to Er [28, 33]. On the other hand, the defect density also affects the binding energy.

3.2. Electrical characteristics

The corrected capacitance-voltage (C-V) and conductance-voltage (G/ω-V) characteristics of the RT, 300 °C, 500 °C, 600 °C, 700 °C-Er_2O_3 MOS capacitors were obtained after the series resistance (R_s) correction detailed in Ref. [34] was applied to the measured data. The accumulation-region R_s values were given in Table 2. Decreasing R_s values with frequency are between 30 and 42 Ω for 50 kHz and 8–20 Ω for 1 MHz. The series resistance values for 500 °C-Er_2O_3 p-MOS produced with RF-magnetron sputtering were found in the range of 59 (50 kHz)-245 (1 MHz) Ω by Morkoc et al. [35] The relatively lower R_s values in this study are indicative of low signal losses during measurement. The R_s values are similar to the data obtained from Yb_2O_3 n-MOS capacitor [21].

The C-V characteristics of the Er_2O_3 MOS capacitors taken in the range of -10 - 15 V are given in Fig. 10. The electrical properties of a MOS capacitor are affected from many parameters such as oxide/Si interface, oxide-interface trap densities, external bias, etc. The border traps and interface states that can exhibit frequency-dependent behaviour and are located very close to the interface may contribute to the

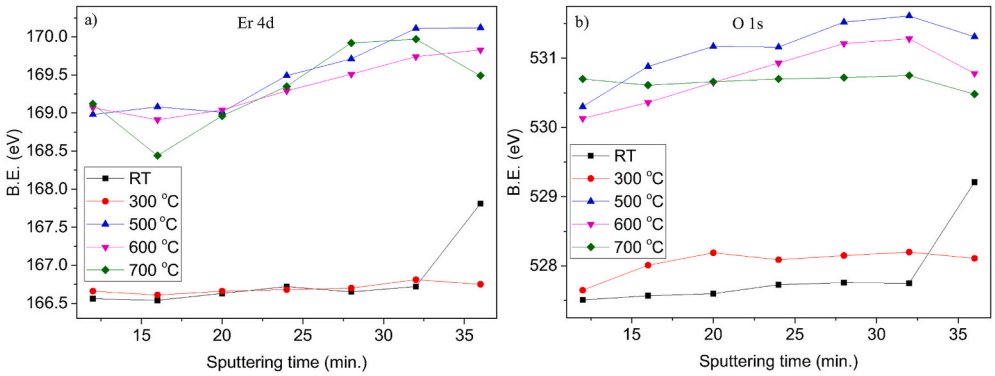

Fig. 8. Depth-dependent binding energy (B.E.) variation: a) Er 4d, b) O 1s.

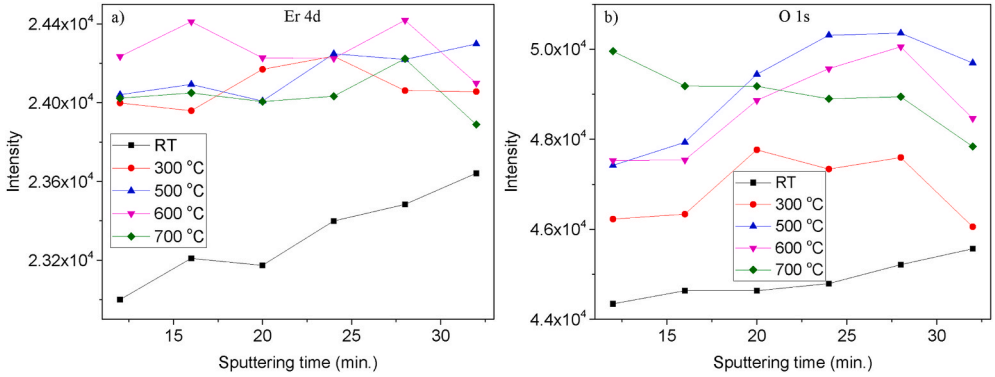

Fig. 9. Depth-dependent signal intensity for a) Er 4d, b) O 1s.

measured capacitance [34]. On the other hand, flat band voltage (V_{fb}) deviates from its ideal value due to trap charges within the structure. The effective oxide charge density (Q_{eff}) is given with below expression [36]:

$$Q_{eff} = \frac{C_{ox}(W_{ms} - V_{fb})}{qA} \quad (1)$$

where C_{ox} is the oxide capacitance, W_{ms}, the metal-semiconductor work function, q is the electric charge and A is the capacitor area (1.767×10^{-2} cm^{-2}). The Q_{eff} values of the Er_2O_3 MOS capacitors were given in Fig. 11. Negative charges are trapped more in the oxide layer than positives in all MOS capacitors. The Q_{eff} values can be given in descending order as RT>300 °C>600 °C>500 °C>700 °C. The Q_{eff} varied from -4.9×10^{11} cm^{-2} to - -31.6×10^{11} cm^{-2}. Obtaining the lowest Er-M content at 500 °C indicates that the lowest Q_{eff} values will also be observed in this sample. However, a slightly higher Si-Si content at 700 °C shifted the flat band voltage to lower negative values, resulting in lower Q_{eff} values. Q_{eff} values did not show great variation depending on frequency at annealing temperatures of 300 °C, 500 °C, 700 °C compared to RT and 600 °C. These results may indicate that the effect of border traps on the electrical characteristics at these annealing temperatures is more limited with respect to RT and 600 °C. The interface trap charge density (N_{it}) was calculated from the following formula based on the single frequency approximation [37]:

$$N_{it} = \frac{2}{qA} \frac{G_{max}/\omega}{\left(\frac{G_{max}}{\omega C_{ox}}\right)^2 + \left(1 - \frac{C_m}{C_{ox}}\right)^2} \quad (2)$$

where ω is the angular frequency, G_{max} is the maximum conductance given in Table 2, and C_m is the capacitance corresponding to maximum conductance. The N_{it} values ranged from 2.6×10^{11}–28.0×10^{11} $eV^{-1}cm^{-2}$ and given in Fig. 12. The interface state density was found to be in the range of 8.46×10^{11}–11.0×10^{11} $eV^{-1}cm^{-2}$ for 500 °C-Er_2O_3/p-Si [35]. The N_{it} values were found to be lower for the same annealing temperature in this study, which means that the formation of the interface is better controlled during the production process. The interface trap density decreases continuously with increasing A.C. voltage frequency in the SiO_2 based devices because these states can not find enough time to follow the signal [38]. N_{it} values can be given in descending order as RT>300 °C>500 °C>600 °C>700 °C and tend to decrease with increasing annealing temperature. It can be said that the interface state density fluctuates depending on frequency. Although the frequency-dependent change in the N_{it} values for RT is larger compared to other annealing temperature, it is not to the extent that it can lead to large differences between the measured/corrected accumulation-region capacitances. N_{it} values can be said to be almost constant for the annealing temperatures of 300 °C, 500 °C, 600 °C, 700 °C. The fact that N_{it} values do not decrease continuously with increasing frequency may be related to the lifetimes of the states. The relaxation time being close to each other may result in no significant change depending on the frequency. Although the interface state density is high for RT, no deformation was observed in the accumulation, depletion and inversion regions of the C-V curve (Fig. 10a). The inversion-region capacitance decreased with increasing negative voltage due to deep depletion for the 300 °C-Er_2O_3 MOS capacitor. The inversion regions of the 500 °C, 600 °C, 700 °C-Er_2O_3 MOS capacitors degraded due to the frequency-dependent charges. It can be said that the inversion-region capacitance values tend to decrease with increasing frequency. There are deformations in the depletion and inversion regions of the 500 °C-Er_2O_3 based device due to the oxide and interface traps (Fig. 10c).

The dielectric constant values (ε) were calculated from the well-known expression, $\varepsilon = C_{ox}d/\varepsilon_o A$, and the values were given in

Table 2
Electrical parameters of the Er_2O_3 MOS capacitor.

Temp. (°C)	Freq. (kHz)	R_s (Ω)	ε	G_{max} (S)	φ_B(eV)	$N_d \times 10^{15}$ (cm^{-3})	E_F (eV)
RT	50	42	15.3	1.68×10^{-4}	0.48	10.0	0.201
	100	35	15.1	3.24×10^{-4}	1.17	11.0	0.198
	250	27	15.0	7.70×10^{-4}	1.83	11.9	0.196
	500	25	14.9	1.40×10^{-3}	1.05	10.3	0.200
	750	21	14.8	1.94×10^{-3}	2.85	12.2	0.196
	1000	20	14.8	2.36×10^{-3}	3.16	10.4	0.200
300	50	30	10.2	3.58×10^{-5}	3.29	16.3	0.188
	100	23	10.1	7.11×10^{-5}	3.40	16.4	0.188
	250	17	10.1	1.85×10^{-4}	3.32	16.1	0.189
	500	16	10.1	3.46×10^{-4}	3.65	16.2	0.188
	750	14	10.1	4.98×10^{-4}	3.61	16.1	0.189
	1000	14	10.1	6.90×10^{-4}	3.16	16.3	0.188
500	50	36	17.4	1.08×10^{-4}	1.21	20.2	0.183
	100	25	17.1	1.77×10^{-4}	1.21	16.6	0.188
	250	15	16.9	4.14×10^{-4}	1.30	11.8	0.196
	500	12	16.8	7.13×10^{-4}	1.20	10.7	0.199
	750	10	16.9	1.00×10^{-3}	1.24	10.0	0.201
	1000	8	17.2	1.27×10^{-3}	1.17	11.2	0.198
600	50	40	13.4	3.49×10^{-5}	0.71	2.4	0.237
	100	32	13.2	1.03×10^{-4}	1.65	2.7	0.233
	250	23	13.1	2.64×10^{-4}	1.76	2.7	0.234
	500	20	13.1	4.92×10^{-4}	1.90	2.9	0.232
	750	18	13.1	7.03×10^{-4}	2.07	3.0	0.231
	1000	17	13.3	8.69×10^{-4}	2.59	3.5	0.227
700	50	39	14.9	3.95×10^{-5}	0.46	4.3	0.222
	100	29	14.7	8.35×10^{-5}	0.37	4.4	0.222
	250	19	14.6	2.33×10^{-4}	0.36	3.9	0.224
	500	15	14.5	4.65×10^{-4}	0.32	3.9	0.224
	750	14	14.6	7.08×10^{-4}	0.33	3.7	0.225
	1000	11	14.8	1.10×10^{-3}	0.35	3.7	0.226

Table 2. The dielectric constant of RT-Er_2O_3 film was found higher than other annealing temperatures except 500 °C. The two most possible of this condition are: i) RT-Er_2O_3 film contains the hydroxyl species, and the permittivity of the water molecules is high ($\varepsilon \cong$ for 20 °C). ii) The interface states may contribute to the measured capacitance. However, the high erbium silicate content observed at the interface may have caused a decrease in the dielectric constant at RT and 600 °C-Er_2O_3. The lowest dielectric constant was obtained from the 300 °C-Er_2O_3 MOS capacitor, which is likely due to the high Er-M content (Fig. 5). Observing the lowest oxygen deficient bond content at both the interface and the oxide layer at 500 °C may have achieved the highest dielectric constant from this annealing temperature. The dielectric constant for the Er_2O_3 film has been reported in the range of 10.1–14.4 in various studies [6,8,39–43]. The values varied from 10.1 to 17.4 in this study are compatible with literature.

The barrier height (φ_B) is an important parameter that indicates which acceptor-like or donor-type interface states are more effective on the electrical characteristics. A MOS capacitor can be considered as a parallel plate capacitor, which has dielectric between the two conductors. Thus, dopant concentration (N_d), Fermi energy level (E_F) and barrier height (φ_B) parameters can be determined from C^{-2}-V characteristics. The depletion-region capacitance (C_{dep}) is expressed as follows [44]:

$$\frac{1}{C_{dep}^2} = \frac{2(V_{bi} + V)}{qN_d\varepsilon_s A^2} \tag{3}$$

where ε_s is the semiconductor dielectric constant, V is the gate voltage, and V_{bi} is the built-in potential, defined by the point at which the linear parts of the C^{-2}-V curves intersect the voltage axis (Fig. 13). N_d is found from the slope of line (S):

$$S = \frac{2}{qN_d\varepsilon_s A^2} \tag{4}$$

The image charges-induced potential causes the decreasing in the barrier height expressed as follows:

$$\Delta\varphi_b = \left[\frac{q\varepsilon_{max}}{4\pi\varepsilon_s}\right]^{1/2} \tag{5}$$

where ε_{max} is the maximum electric field. The barrier height is given with

$$\varphi_B = V_{bi} + \frac{k_B T}{q} + E_F - \Delta\varphi_b = V_{bi} + \frac{k_B T}{q} + \frac{k_B T}{q} ln\left(\frac{N_c}{N_d}\right) - \Delta\varphi_b \tag{6}$$

[44–46]. Increasing barrier height in an n-type semiconductor indicates that acceptor-like interface states are more effective in electrical parameters than donor-like interface states. While the donor-like interface states move the flat band voltage to larger negative voltages, the acceptor-like interface states shifts to larges positive voltages. The frequency-dependent change of the barrier height is similar for RT and 300 °C-Er_2O_3 MOS capacitor. The φ_B values of RT, 300 °C and 500 °C-Er_2O_3 MOS devices do not show a continuous increase or decrease, pointing out that the superiority of the acceptor-like and donor-like interface states relative to each other changes continuously depending on the frequency. The acceptor-like interface states have been superior to those of donor-like with the increasing frequency in the 600 °C-Er_2O_3 MOS capacitor, and the φ_B has increased continuously. The barrier height has been continuously decreased up to 50 kHz and increased after this frequency in the 700 °C-Er_2O_3 MOS capacitor. The donor-like interface states in the low frequency region (≤500 kHz), and the acceptor-like interface states in the high frequency region played an effective role on the electrical characteristics. While the highest φ_B values are observed at 300 °C-Er_2O_3 MOS capacitor, 700 °C-Er_2O_3 based device has the lowest values.

3.3. Relationship between structural properties and electrical characteristics

The binding energies of the Er 4d spectra taken from the RT and 300 °C-Er_2O_3/n-Si are quite close to each other (Fig. 8a). These results are an indication that oxygen prefers to bond in the films at a similar rate at both annealing temperature. The binding energy of Er 4d at the Er_2O_3/n-Si interface for RT is higher than that of 300 °C. The erbium silicate content at the RT-Er_2O_3/n-Si interface is ~25% and higher than 300 °C. Since the electronegativity of Si (χ_{Si}=1.9) is higher than that of

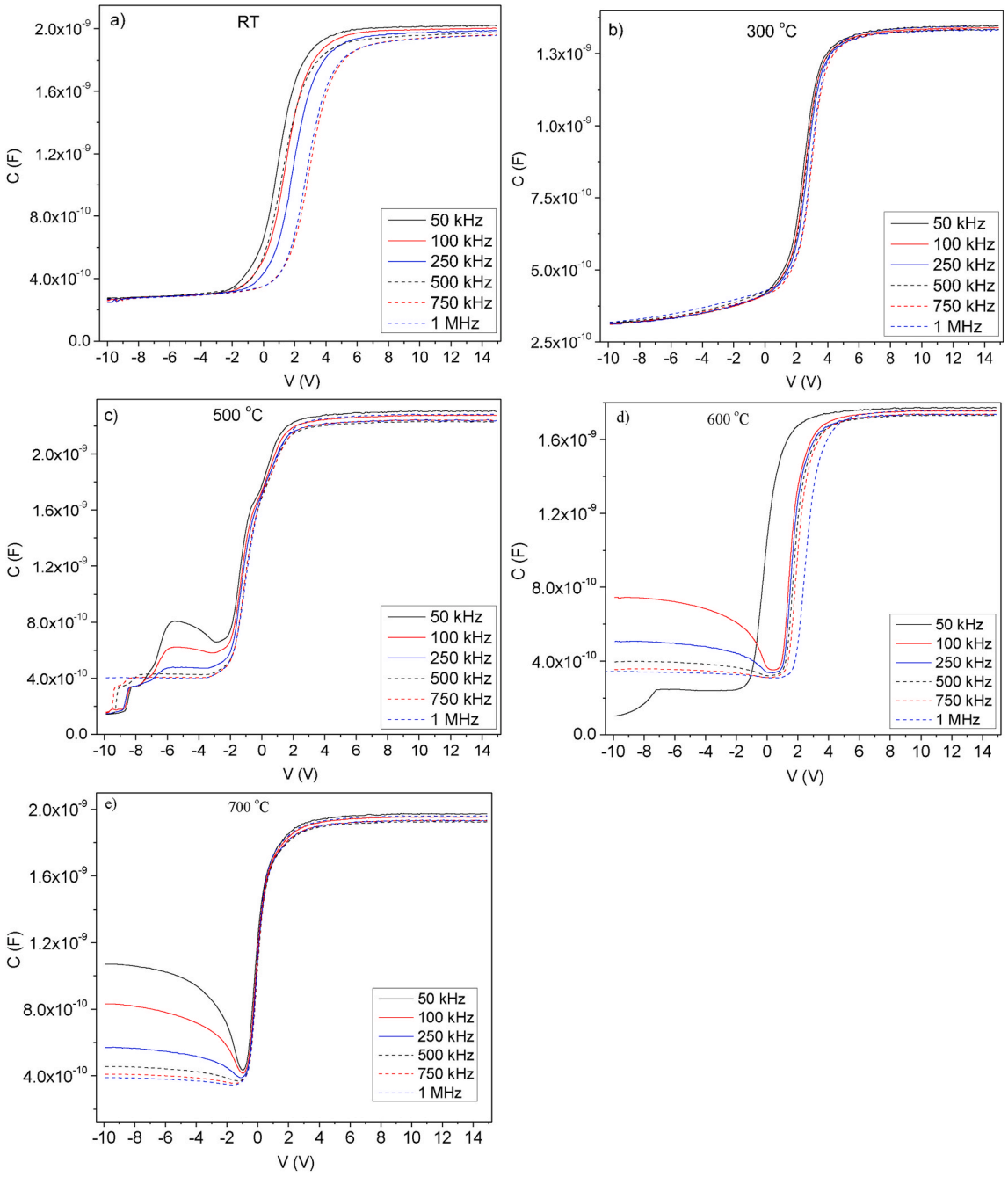

Fig. 10. C-V characteristics of the Er_2O_3 MOS capacitors: a) RT, b) 300 °C, c) 500 °C, d) 600 °C, e) 700 °C.

Er ($\chi_{Er} = 1.24$), Er 4d binding energy in RT may have shifted to higher values compared to 300 °C [33]. Similar situation is valid for the binding energies of O 1s spectra taken from the interface (36 min) at RT and 300 °C. The oxygen atomic concentration in the film for 300 °C is lower than that of RT, resulting in higher Er-Er oxygen deficient bond content in the 300 °C-Er_2O_3 film. The results in Fig. 5 support this interpretation. The binding energy of the Er-O-Er peak in Er 4d spectra in both RT and 300 °C was almost at a constant value depending on depth up to interface. These results show that the bonding ratio between O and Er does not change much, in layers (12–32 min) in the film. The decrease in oxygen concentration can be associated with the increase in Q_{eff} values as can be seen from the results in Figs. 3 and 11. Although the oxygen concentration is higher in the film for RT compared to 300 °C and 600 °C, the reason for the highest Q_{eff} values observed at this annealing temperature may be the difference of the structural property of the interface and hydroxyl species observed in the structure. Oxygen content at 300 °C-Er_2O_3/n-Si interface is more than those of RT and 600 °C-Er_2O_3/n-Si interfaces (Fig. 3). No erbium silicate formation occurred at the 300 °C-Er_2O_3/n-Si interface. The oxygen formed the Er-O-M, Er-O, Si-O and –OH bonds in the film and interface of RT-Er_2O_3/n-Si structure. Therefore, there are more Er-Er, Er-Si and hydrogen-related defects in RT-interface compared to that of 300 °C. These defective bonds may cause the flat band voltage to shift to larger positive values. Production-origin Er-Er, Er-Si oxygen deficient bonds and hydrogen based bonds may act as negative charge trap centers [9].

The highest oxygen content was obtained from the 500 °C-Er_2O_3/n-Si structure. Therefore, it is expected that there will be less Er-M oxygen deficient bond content in this structure compared to the others, and the data in Fig. 5 support this interpretation. The binding energy of the Er 4d spectrum at 500 °C tends to increase with increasing depth due to

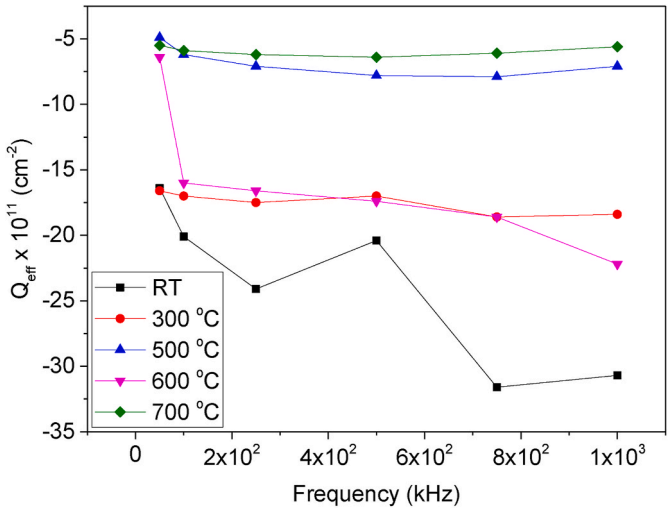

Fig. 11. Frequency-dependent Q_{eff} values for the Er_2O_3 MOS capacitors.

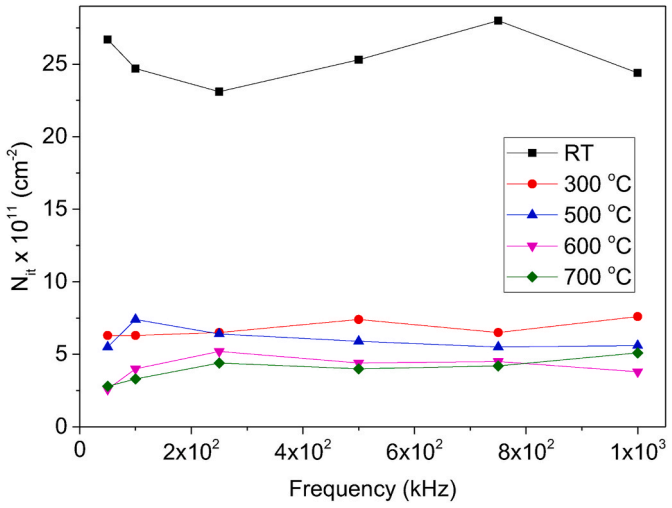

Fig. 12. Frequency-dependent N_{it} values for the Er_2O_3 MOS capacitors.

oxygen bonding to Er atoms. Erbium silicate formation at the 500 °C-Er_2O_3/n-Si interface is around 3%. 500 °C-Er_2O_3/n-Si structure may contain less Er-M oxygen deficient bonds compared to RT, 300 °C, 600 °C, resulting in lower Q_{eff} values in 500 °C-Er_2O_3 MOS capacitor.

As seen from Fig. 8a, the binding energy of the Er 4d spectrum in the structure of 600 °C-Er_2O_3/n-Si decreased slightly compared to that of 500 °C. Therefore, it can be said that Er-O bonding at 600 °C is less compared to 500 °C, which is supported by the results given in Fig. 5. Although the content of Er-M at 600 °C in the first four layers (12–24 min) was lower compared to the structure annealed at RT and 300 °C, it increased significantly afterwards (Fig. 5). The average Er-Er content is slightly lower at 600 °C (0.179) compared to 300 °C (0.191) within the film, resulting in less Q_{eff} value in three layers of the 600 °C-Er_2O_3/n-Si (12–20 min). It is seen from the O 1s spectra results obtained from the RT and 600 °C interfaces that the erbium silicate content is higher at 600 °C, although the Er-O-Er content is the same at these annealing temperatures (Table 1). The reader should remember here that the lowest oxygen concentration at the interface is at 600 °C. These results show that there are more Si-Si, Er-Si, Er-Er deficient bonds at 600 °C-Er_2O_3/n-Si interface compared to that of RT. As seen in Fig. 5, the content of Er-M is higher in the interface at 600 °C compared to RT. The Er-Si content is lower at 600 °C-Er_2O_3/n-Si interface compared to that of RT, resulting in higher Er-Er content at 600 °C with respect to RT. On the other hand, Si-Si content, which can act as positive charge trap center, is also higher at 600 °C compared to RT (Table 1). Si-Si oxygen deficient bonds at 600 °C are may play a dominant role on electrical characteristics compared to Er-Er, which likely acts as a negative load trap center. The more positive charge traps and lack of the hydrogen based defects in the 600 °C-Er_2O_3/n-Si with respect to RT-Er_2O_3/n-Si provide the less Q_{eff} value.

The oxygen atomic concentration at 700 °C is higher than all annealing temperatures except 500 °C. For this reason, the content of Er-M was generally lower than other annealing temperatures other than 500 °C, which may be related to the interface formation. The Si atomic concentration at interface is very low in both samples, resulting in low signal intensity. Therefore, it will not be healthy to separate Er-Si and Si-Si bonds in Si 2p spectra taken from the interfaces. However, the intensity of the Si 2p at the interface is slightly higher at 700 °C than 500 °C. This indicates that the Er-Si and/or Si-Si oxygen deficient bonds at the interface are higher at 700 °C than at 500 °C. The slightly more positive charge trap centers at the interface may have shifted the flat band voltage to larger negative voltages, leading to lower Q_{eff} values. Although more oxygen deficient bonds are observed in the oxide at 700 °C compared to 500 °C, that the interface traps play a more effective role on the electrical characteristics compared to the oxide trap charges enabled the flat band voltage to be observed at lower values compared to all other annealing temperatures.

4. Conclusion

The structural modifications of the Er_2O_3 films grown on n-type Si substrate under different annealing temperatures are investigated in detail and a connection is established between the changes and electrical characteristics in this study. The lowest particle size value was obtained from the RT-Er_2O_3 film, while it received similar values in the 300 °C–700 °C temperature range. The bonded oxygen species was only observed in the RT-Er_2O_3/n-Si structure. The erbium silicate contents in the interface of the RT and 600 °C-Er_2O_3/n-Si structures were found to be higher than the others. No erbium silicate formation was observed at the 300 °C-Er_2O_3/n-Si interface. That the signal intensity of the Er 4d spectrum increased with the annealing temperature of 300 °C and the almost constant values were observed with increasing temperature mean that the crystallization improved with 300 °C and did not show a big change with increasing annealing temperature. These XPS results are consistent with XRD data. No major differences were observed between the measured and corrected capacitance values due to the low series resistance values. The highest dielectric constant value was obtained from the 500 °C-Er_2O_3 structure due to possible reason of the lowest content of the oxygen deficient bond. It has been found that Q_{eff} values tend to increase with decreasing oxygen concentration. Therefore, it was concluded that the production-origin Er-Er oxygen deficient bonds may act as negative charge trap center. It was found that it is not possible to interpret the Q_{eff} values by only determining the oxygen deficient bond contents in the oxide layer, because it was concluded that Er-Er and Si-Si oxygen deficient bonds formed in the interface play a very effective role on the electrical characteristics in many cases. It was not possible to reach a general judgment that Er-Si defective bonds most likely behave like a negative or positive charge trap center with the results of this study.

It is a very interesting result that the electrical characteristics deteriorate as the Q_{eff} and N_{it} decrease. These results indicate that the defects are not permanently repaired with annealing. On the other hand, the leakage current in the devices produced with amorphous films may be lower than those fabricated with the crystallized films. The opposite may also be the case. Although the thickness used in the study is not enough to cause a problem in terms of leakage current, this disadvantage is the reason for the negative effects of annealing on electrical characteristics. Further studies should be directed at reducing defect concentrations at low annealing temperatures. For this purpose, it is important to examine

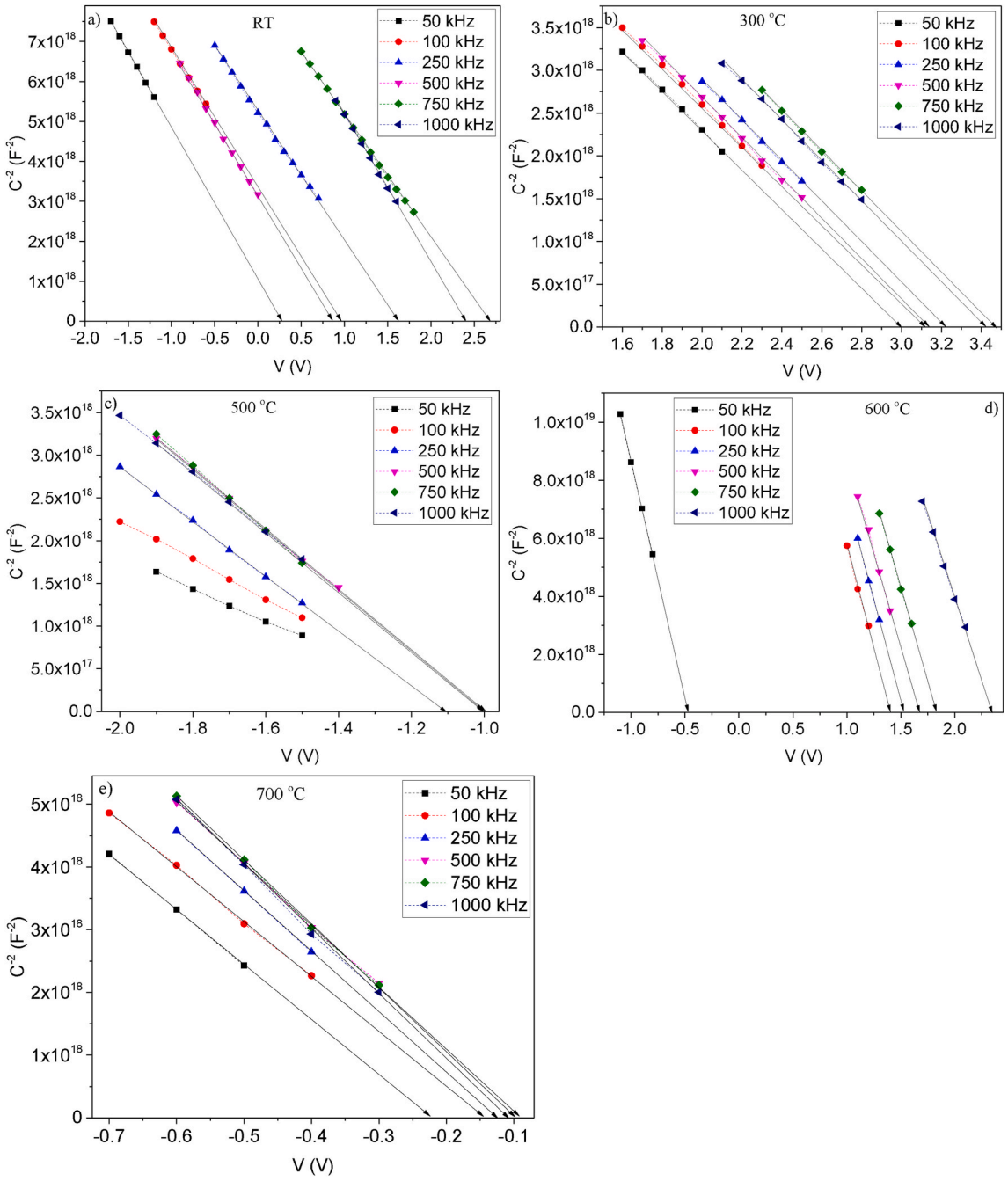

Fig. 13. C^{-2}-V characteristics of the Er_2O_3 MOS capacitors: a) RT, b) 300 °C, c) 500 °C, d) 600 °C, e) 700 °C.

the annealing at low temperatures under oxygen in detail.

CRediT authorship contribution statement

Aysegul Kahraman: Conceptualization, Validation, Writing – original draft, Formal analysis. **Berk Morkoc:** Investigation, Validation. **Ercan Yilmaz:** Conceptualization, Validation, Formal analysis, Investigation, Resources, Writing – original draft, Project administration, Funding acquisition.

Declaration of competing interest

The authors declare that they have no known competing financial interests or personal relationships that could have appeared to influence the work reported in this paper.

Acknowledgments

This work is supported by the Scientific and Technological Research Council of Turkey (TUBITAK) under ARDEB1001- Scientific and Technological Research Projects Support Program (Contract Number: 117R054) and also supported in part by the Presidency of Turkey, Presidency of Strategy and Budget under Contract Number: 2016K12-2834.

References

[1] J. Gao, G. He, Z. Sun, H. Chen, C. Zheng, P. Jin, D. Xiao, M. Liu, Modification of electrical properties and carrier transportation mechanism of ALD-derived HfO_2/Si gate stacks by Al_2O_3 incorporation, J. Alloys Compd. 667 (2016) 352–358.

[2] A. Kahraman, E. Yilmaz, Proposal of alternative sensitive region for MOS based radiation sensors: Yb_2O_3, J. Vac. Sci. Technol. A Vac. Surf. Film. 35 (2017), 061511.

[3] R. Lok, S. Kaya, H. Karacali, E. Yilmaz, The Co-60 gamma-ray irradiation effects on the Al/$HfSiO_4$/p-Si/Al MOS capacitors, Radiat, Phys. Chem. 141 (2017) 155–159.

[4] L. Yan, W. He, X. Liang, C. Liu, X. Lu, C. Luo, A. Zhang, R. Tao, Z. Fan, M. Zeng, H. Ning, G. Zhou, X. Lu, J. Liu, Oxygen incorporated solution-processed high-: κ La_2O_3 dielectrics with large-area uniformity, low leakage and high breakdown field comparable with ALD deposited films, J. Mater. Chem. C. 8 (2020) 5163–5173.

[5] Y. Zhu, Z. Fang, Y. Liu, Structural and optical properties of Er_2O_3 films, J. Rare Earths 28 (2010) 752–755.

[6] V. Mikhelashvili, G. Eisenstein, F. Edelman, R. Brener, N. Zakharov, P. Werner, Structural and electrical properties of electron beam gun evaporated Er_2O_3 insulator thin films, J. Appl. Phys. 95 (2004) 613–620.

[7] K.H. Goh, A.S.M.A. Haseeb, Y.H. Wong, Lanthanide rare earth oxide thin film as an alternative gate oxide, Mater. Sci. Semicond. Process. 68 (2017) 302–315.

[8] F.-H. Chen, J.-L. Her, Y.-H. Shao, Y.H. Matsuda, T.-M. Pan, Structural and Electrical Characteristics of High-κ Er2O3 and Er2TiO5 Gate Dielectrics for A-IGZO Thin-Film Transistors, vol. 8, 2013, pp. 1–5.

[9] G.S. Ristić, M.M. Pejović, A.B. Jakšić, Physico-chemical processes in metal–oxide–semiconductor transistors with thick gate oxide during high electric field stress, J. Non-Cryst. Solids 353 (2007) 170–179.

[10] X.J. Zheng, L. He, Y.C. Zhou, M.H. Tang, Effects of europium content on the microstructural and ferroelectric properties of $Bi_{4-x}Eu_xTi_3O_{12}$ thin films, Appl. Phys. Lett. 89 (2006) 10–13.

[11] A.J. Lelis, T.R. Oldham, H.E. Boesch, F.B. McLean, The nature of the trapped hole annealing process, IEEE Trans. Nucl. Sci. 36 (1989) 1808–1815.

[12] A.J. Lelis, H.E. Boesch, T.R. Oldham, F.B. McLean, Reversibility of trapped hole annealing, IEEE Trans. Nucl. Sci. 35 (1988) 1186–1191.

[13] T.R. Oldham, Switching oxide traps in radiation effects and soft errors in integrated circuits and electronic devices, in: R.D. Schrimpf, D.M. Fleetwood (Eds.), Singapore: World Scientific, 2004, pp. 297–319.

[14] C. Henkel, S. Abermann, O. Bethge, G. Pozzovivo, P. Klang, M. Stöger-Pollach, E. Bertagnolli, Schottky barrier SOI-MOSFETs with high-k La_2O_3/ZrO_2 gate dielectrics, Microelectron. Eng. 88 (2011) 262–267.

[15] S. Regnery, R. Thomas, P. Ehrhart, R. Waser, $SrTa_2O_6$ thin films for high- K dielectric applications grown by chemical vapor deposition on different substrates, J. Appl. Phys. 97 (2005), 073521.

[16] S.D. Cho, J.Y. Lee, K.W. Paik, Effects of particle size on dielectric constant and leakage current of epoxy/barium titanate ($BaTiO_3$) composite films for embedded capacitors, Adv. Electron. Mater. Packag. (2001) 63–68.

[17] K. McKenna, A. Shluger, V. Iglesias, M. Porti, M. Nafría, M. Lanza, G. Bersuker, Grain boundary mediated leakage current in polycrystalline HfO_2 films, Microelectron. Eng. 7 (2011) 1272–1275.

[18] H. Kim, S. Yang, K. Park, P. Shanmugam, K.Y. Kwon, Leakage current analysis depends on grain size variation in zinc oxide thin film transistor, 2013 ECS - the electrochemical society, ECS Meeting Abstracts, 76, 2-MA2013.

[19] A. Kahraman, E. Yilmaz, A. Aktag, S. Kaya, Evaluation of radiation sensor aspects of Er_2O_3 MOS capacitors under zero gate bias, IEEE Trans. Nucl. Sci. 63 (2016) 1284–1293.

[20] S. Kaya, E. Yilmaz, Modifications of structural, chemical, and electrical characteristics of Er_2O_3/Si interface under Co-60 gamma irradiation, Nucl. Instrum. Methods Phys. Res. Sect. B Beam Interact. Mater. Atoms 418 (2018) 74–79.

[21] A. Kahraman, H. Karacali, E. Yilmaz, Impact and origin of the oxide-interface traps in Al/Yb_2O_3/n-Si/Al on the electrical characteristics, J. Alloys Compd. 825 (2020), 154171.

[22] A.J. Brown, Spectral curve fitting for automatic hyperspectral data analysis, IEEE Trans. Geosci. Rem. Sens. 44 (2006) 1601–1607.

[23] B. Vincent Crist, Handbook of Monochromatic XPS Spectra, Demo Version, XPS International, LLC, 1999, p. 87.

[24] J.I. Langford, A.J.C. Wilson, Scherrer after sixty years: a survey and some new results in the determination of crystallite size, J. Appl. Crystallogr. 11 (1978) 102–113.

[25] M. Ding, Y. Cheng, X. Liu, X. Li, Total dose response of hafnium oxide based metal-oxide-semiconductor structure under gamma-ray irradiation, IEEE Trans. Dielectr. Electr. Insul. 21 (2014) 1792–1800.

[26] R.M. Todi, A.P. Warren, K.B. Sundaram, K.R. Coffey, X-ray photoelectron spectroscopy analysis of oxygen annealed radio frequency sputter deposited SiCN thin films, J. Electrochem. Soc. 153 (2006) G640–G643.

[27] S. Ahmad Kamil, J. Chandrappan, J. Portoles, P. Steenson, G. Jose, Local structural analysis of erbium-doped tellurite modified silica glass with X-ray photoelectron spectroscopy, Mater. Res. Express 6 (2019), 086220.

[28] C.-H. Kao, H. Chen, Y.T. Pan, J.S. Chiu, T.-C. Lu, The characteristics of the high-K Er_2O_3 (erbium oxide) dielectrics deposited on polycrystalline silicon, Solid State Commun. 152 (2012) 504–508.

[29] T.M. Pan, C.H. Chen, Y.H. Hu, H.C. Wang, J.L. Her, Comparison of structural and electrical properties of Er_2O_3 and $ErTi_xO_y$ charge-trapping layers for InGaZnO thin-film transistor nonvolatile memory devices, IEEE Electron. Device Lett. 37 (2016) 179–181.

[30] H. Wen, J. He, J. Hong, S. Jin, Z. Xu, H. Zhu, J. Liu, G. Sha, F. Yue, Y. Dan, Efficient Er/O-doped silicon light-emitting diodes at communication wavelength by deep cooling, Adv. Opt. Mater. 8 (2020), 2000720.

[31] S. Gokhale, S. Mahamuni, S.V. Deshmukh, V.J. Rao, A.S. Nigavekar, S.K. Kulkarni, Photoemission and x-ray diffraction study of the Er Si(111) interface, Surf. Sci. 237 (1990) 127–134.

[32] M. Losurdo, M.M. Giangregorio, P. Capezzuto, G. Bruno, G. Malandrino, I. L. Fragalà, L. Armelao, D. Barreca, E. Tondello, Structural and optical properties of nanocrystalline Er_2O_3 thin films deposited by a versatile low-pressure MOCVD approach, J. Electrochem. Soc. 155 (2008) G44–G50.

[33] J. Zhang, H. Wong, D. Yu, K. Kakushima, H. Iwai, X-ray photoelectron spectroscopy study of high-k CeO_2/La_2O_3 stacked dielectrics, AIP Adv. 4 (2014), 117117.

[34] A. Kahraman, U. Gurer, R. Lok, S. Kaya, E. Yilmaz, Impact of interfacial layer using ultra-thin SiO_2 on electrical and structural characteristics of Gd_2O_3 MOS capacitor, J. Mater. Sci. Mater. Electron. 29 (2018) 17473–17482.

[35] B. Morkoc, A. Kahraman, A. Aktag, E. Yılmaz, Electrical parameters of the erbium oxide MOS capacitor for different frequencies, Celal Bayar Univ. J. Sci 15 (2019) 139–143.

[36] Y. Zeng, Tailored Al_2O_3/4H-SiC Interface Using Ion Implantation, M.S. thesis, Department of Integrated Circuits and Devices, KTH Royal Institute of Technology School, Stockholm, Sweden, 2011, p. 42.

[37] C.C. Coleman, W.A. Hill, A single-frequency approximation for interface-state density determination, Solid-State Electronics 23 (1980) 987–993.

[38] H. Xiao, S. Huang, Frequency and voltage dependency of interface states and series resistance in Al/SiO_2/p-Si MOS structure, Mater. Sci. Semicond. Process. 13 (2010) 395–399.

[39] A. Kahraman, S.C. Deevi, E. Yilmaz, Influence of frequency and gamma irradiation on the electrical characteristics of Er_2O_3, Gd_2O_3, Yb_2O_3, and HfO_2 MOS-based devices, J. Mater. Sci. 55 (2020) 7999–8040.

[40] M. Losurdo, M.M. Giangregorio, P. Capezzuto, G. Bruno, R.G. Toro, G. Malandrino, I.L. Fragalà, L. Barreca, E. Tondello, A.A. Suvorova, D. Yang, E.A. Irene, Multifunctional nanocrystalline thin films of Er_2O_3: interplay between nucleation kinetics and film characteristics, Adv. Funct. Mater. 17 (2007) 3607–3612.

[41] M. Losurdo, M.M. Giangregorio, G. Bruno, D. Yang, E.A. Irene, A.A. Suvorova, M. Saunders, Er_2O_3 as a high- K dielectric candidate, Appl. Phys. Lett. 91 (2007) 89–92.

[42] S. Chen, Y.Y. Zhu, R. Xu, Y.Q. Wu, X.J. Yang, Y.L. Fan, F. Lu, Z.M. Jiang, J. Zou, Superior electrical properties of crystalline Er_2O_3 films epitaxially grown on Si substrates, Appl. Phys. Lett. 88 (2006) 8–11.

[43] F.C. Chu, Y.J. Tsai, S.Y. Liao, C.S. Huang, R.M. Lin, S.F. Yu, S. Sen Ren, Improved gate leakage and microwave performance by inserting a thin erbium oxide layer on AlGaN/GaN/Silicon HEMT structure, 2012, Int. Conf. Compd. Semicond. Manuf. Technol. Cs Mantech (2012) 3–6, 2012.

[44] S.M. Sze, K.K. Ng, Physics of Semiconductor Devices, Wiley-Interscience, New Jersey, USA, 2007, p. 812.

[45] W. Bachir Bouiadjra, A. Saidane, A. Mostefa, M. Henini, M. Shafi, Effect of nitrogen incorporation on electrical properties of Ti/Au/GaAsN Schottky diodes, Superlattice. Microst. 71 (2014) 225–237.

[46] J.-P. Colinge, C.A. Colinge, Physics of Semiconductor Devices, Kluwer Academic Publishers, USA, 2002, p. 436.